

Transport, Magnetic and Vibrational Properties of Chemically Exfoliated Few Layer Graphene

Bence G. Márkus,¹ Ferenc Simon,¹ Julio C. Chacón-Torres,² Stephanie Reich,² Péter Szirmai,³ Bálint Náfrádi,³ László Forró,³ Thomas Pichler,⁴ Philipp Vecera,⁵ Frank Hauke,⁵ and Andreas Hirsch⁵

¹*Department of Physics, Budapest University of Technology and Economics, POBox 91, H-1521 Budapest, Hungary*

²*Institute of Experimental Physics, Freie Universität Berlin, Arnimallee 14, 14195 Berlin, Germany*

³*Institute of Physics of Complex Matter, FBS Swiss Federal Institute of Technology (EPFL), CH-1015 Lausanne, Switzerland*

⁴*Faculty of Physics, University of Vienna, Strudlhofgasse 4, A-1090 Vienna, Austria*

⁵*Department of Chemistry and Pharmacy and Institute of Advanced Materials and Processes (ZMP), University of Erlangen-Nuremberg, Henkestrasse 42, 91054 Erlangen, Germany*

We study the vibrational, magnetic and transport properties of Few Layer Graphene (FLG) using Raman and electron spin resonance spectroscopy and microwave conductivity measurements. FLG samples were produced using wet chemical exfoliation with different post-processing, namely ultrasound treatment, shear mixing, and magnetic stirring. Raman spectroscopy shows a low intensity D mode which attests a high sample quality. The G mode is present at 1580 cm^{-1} as expected for graphene. The 2D mode consists of 2 components with varying intensities among the different samples. This is assigned to the presence of single and few layer graphene in the samples. ESR spectroscopy shows a main line in all types of materials with a width of about 1 mT and a g -factor in the range of 2.005 – 2.010. Paramagnetic defect centers with a uniaxial g -factor anisotropy are identified, which shows that these are related to the local sp^2 bonds of the material. All kinds of investigated FLGs have a temperature dependent resistance which is compatible with a small gap semiconductor. The difference in resistance is related to the different grain size of the samples.

I. INTRODUCTION

Novel carbon allotropes gave an enormous boost to condensed-matter and molecular physics at the end of the last century. The process was started with the discovery of fullerenes¹ and carbon nanotubes², but for the biggest breakthrough we had to wait until 2004³. Since its discovery graphene became one of the most important materials in condensed-matter physics. Being the basis of all other novel carbon allotropes^{4,5} (fullerenes, nanotubes, graphite), understanding graphene is crucial. The mechanical and electronic properties of graphene such as high fracture strength, high elasticity, low resistance, high carrier mobility, quantum Hall-effect make it an outstanding material for diverse applications⁶. However, one of the remaining obstacles for the applicability of graphene is mass production with controlled quality and graphene layer size.

High quality graphene can be prepared by mechanical exfoliation (also referred as mechanical cleavage), but only in small amounts on various substrates (maximum available size is still in the scale of microns⁷). Epitaxial growth of graphene on various substrates^{8–10} is an alternative but the up-scalability of this method is limited and the resulting sample qualities needs yet to be improved. On the other hand, with chemical vapor deposition (CVD) high yields are achievable^{11–17} in a poorer quality due to the enormous number of defects. Another problem with the CVD method is that it still requires a substrate. Being a material of an atomically thin layer on a substrate is a serious issue when one would like to apply bulk characterization methods, such as Electron Spin Resonance spectroscopy (ESR) or macroscopic transport measurements (e.g. microwave conductivity). The substrate also has a negative effect on the electronic and vibrational properties of graphene (e.g. electronic interactions, and induced strain). These effects are visible when one tries to compare the results of free-standing graphene¹⁸ with graphene on other substrates:

Si-SiO₂¹⁹, Si-SiO₂ and ITO²⁰, SiC²¹, glass²².

Other ways to create graphene in a mass production is reduction from graphite/graphene oxide (GO) and wet chemical exfoliation from graphite intercalation compounds (GICs) with various solvents. Reduction process is feasible in many chemical and biological routes with different quality of the final product^{23–35}. In general, the quality of final product may vary in a large scale but always contains residual oxygen, missing carbon atoms, free radicals, and dangling bonds therefore one can end up with a thermally metastable material^{36–40}.

Wet chemical or liquid phase exfoliation is the most promising way to mass produce high quality materials without disturbing the effects of the substrate^{41–52}. For the optimal quality of the outcome the effect of solvent⁵³ and the mechanical post-processing has to be examined. Here we report the transport, magnetic and vibrational properties of Wet Chemically Exfoliated (WCEG) Few Layer Graphene (FLG) using microwave conductivity, electron spin resonance and Raman spectroscopies.

II. EXPERIMENTAL

We studied three WCEG species which were prepared by different mechanical routes: ultrasounded (US), shear mixed (SM) and stirred (ST). All kinds were produced from saturate intercalated potassium graphite powder, KC₈ using DMSO solvent for wet exfoliation (full protocol is described in Ref.⁵²). The starting material, SGN18 graphite powder (Future Carbon) and Grade I bulk HOPG (SPI) were taken into comparison. Mechanical post-processing were ultrasound treatment, shear mixing and magnetic stirring. The procedure was done under argon atmosphere. The pristine materials were cleaned under high vacuum (10^{-7} mbar) at 400°C for one hour to get rid of the remaining solvent and impurities. Raman measurements were carried out in a high sensitivity

single monochromator LabRam spectrometer⁵⁴ using 514 nm laser excitation, 50 \times objective with 0.5 mW laser power. For ESR measurements a Bruker Elexsys E580 X-band spectrometer was used. Microwave conductivity measurements were done with the cavity perturbation technique^{55,56} extended with an AFC feedback loop to increase precision⁵⁷. The photographs were taken with a Nikon Eclipse LV150N optical microscope using 5 \times (for FLG) and 10 \times (for SGN18) objectives.

III. RESULTS AND DISCUSSION

To get an insight on which mechanical post production method produces the best quality, the vibrational, electronic and transport properties of the materials have to be investigated. We discuss the Raman, ESR and microwave conductivity results.

A. Raman spectroscopy

Raman spectra of the examined samples are shown in Fig. 1. Namely, the D, G, and 2D Raman modes are presented. The D mode is associated with the presence of defects⁵⁸. The 2D is its overtone. And the G (graphitic) mode is related to tangential motion of carbon atoms and it is the most pronounced in graphite. Solid lines represent Lorentzian fits. In most cases 2D lines are made up of 2 components, namely 2D₁ and 2D₂. In the case of ultrasound preparation the 2D feature can also be well fitted with one single Lorentzian. Parameters of the fitted Lorentzian curves are given in Table I.

The Raman spectrum properties of graphite powder differ from HOPG. This is not an instrumental artifact, positions and widths of peaks in case of graphite strongly depends on morphology and grain size⁵⁹.

514 nm	HOPG	SGN18	US	SM	ST
ν_D	1358.4	1349.8	1355.5	1350.6	1353.9
$\Delta\nu_D$	18.6	15.5	20.0	29.4	14.2
ν_G	1583.3	1579.0	1583.3	1581.6	1582.2
$\Delta\nu_G$	6.9	8.1	9.5	10.6	9.6
ν_{2D_1}	2688.4	2686.2	2696.4	2692.8	2692.4
$\Delta\nu_{2D_1}$	21.4	21.4	25.7	23.7	23.9
ν_{2D_2}	2728.6	2722.8	2727.2	2726.1	2729.0
$\Delta\nu_{2D_2}$	17.1	19.6	14.7	17.4	17.3
ν_{2D}^*			2714.6		
$\Delta\nu_{2D}^*$			29.4		

TABLE I. Parameters of the fitted Lorentzian curves for the D, G, and 2D Raman modes for a 514 nm excitation. ν denotes the position and $\Delta\nu$ the FWHM in cm^{-1} , * stands for single Lorentzian fit.

The D peak is less pronounced when ultrasound sonication or shear mixing was applied in case of exfoliated graphenes.

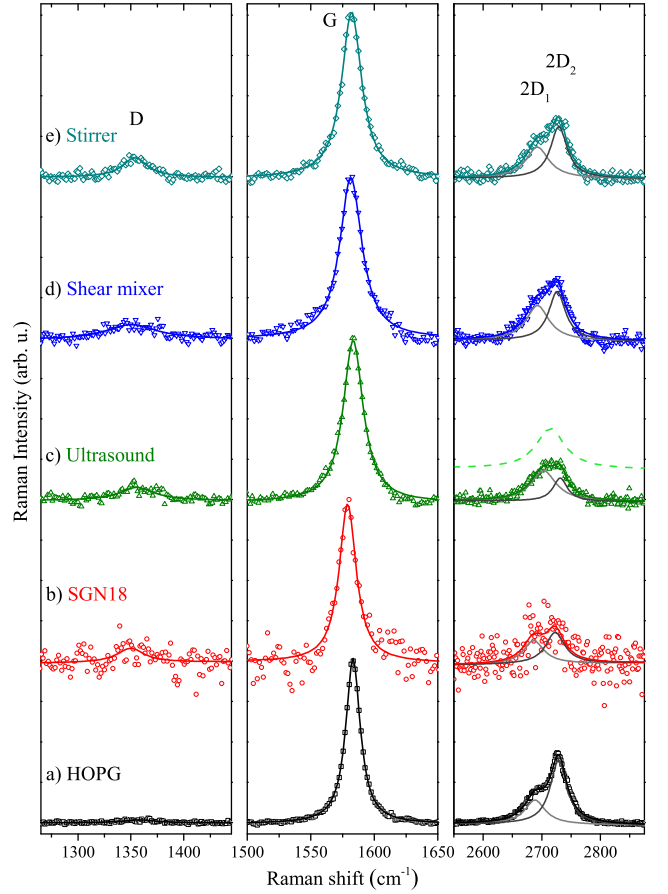


FIG. 1. D, G, 2D Raman modes of the investigated species using 514 nm laser excitation. a) bulk HOPG, b) SGN18 graphite powder, c) ultrasound sonicated exfoliated graphene, d) shear mixed exfoliated graphene, e) stirred exfoliated graphene. Solid color line represents Lorentzian-fits, grey lines denotes the decomposition of the 2D peaks. The dashed green line in case of the ultrasound sample points that the 2D peak can be fitted with one single Lorentzian as well.

The position of the D peak varies between the graphite powder and HOPG. According to mechanically exfoliated and CVD studies^{12,19} the D peak is expected at about 1350 cm^{-1} which is in a good agreement with our results. Both Ferrari and Das²⁰ agree that the intensity of the D peak for single layer material has to be negligible in order to assure a high quality of the material. The ultrasounded and shear mixed samples satisfies this criterion. The D peak is always present in wet chemically exfoliated graphenes^{44,45} but its intensity is flake-size dependent⁵⁰. The wet exfoliation according to the D peak intensity is far better in quality than for reduced GO samples^{23,25,30}.

All our FLG samples have a sharp G peak very close to HOPG (we remind that the starting material is SGN18). The width is about $\sim 2 \text{ cm}^{-1}$ broader than graphite (both powder and bulk). Position of the G mode varies around 1580 cm^{-1} in good agreement with previous studies^{19,20}. The G-line position also depends on the substrate and the number

of layers. According to Ref.¹⁸, the G peak position for the shear mixed and ultrasounded materials are very close to free-standing graphene.

The 2D peak for single layer graphene is expected to be a single, symmetric peak¹⁹. The position of the peak is about 2700 cm^{-1} and shows a variation in the literature^{19,20,41,43}. Width of the peak also varies in a wide scale from 15 up to 40 cm^{-1} . Variations can be explained with the effect of the substrate (samples on substrates always present a narrower peak) and the effect of preparations (strain, compressive forces may apply, and chemicals may remain). Our FLG samples show two components for the 2D line. The position of the lower $2D_1$ peak agrees with previous single layer studies, thus this component is associated with single layer graphene sheets. The $2D_2$ peak position is close to that of graphite. The presence of the $2D_2$ mode can be interpreted as the presence of few layer sheets up to 4 layers. The nominal width of the peaks suggest that we are dealing with single and few layer graphenes unlike in turbostratic graphite (in that case the width of 2D would be about 50 cm^{-1} ¹⁹). Bilayer graphene has a unique 2D peak made up of 4 components¹⁹, which is not present here. In case of the ultrasounded sample, the 2D peak can also be well fitted with one single Lorentzian with a position up to 2715 cm^{-1} .

The amplitude ratios of 2D and G peaks are given in Table III A.

514 nm	HOPG	SGN18	US	SM	ST
I_{2D_1}/I_G	0.21	0.17	0.21	0.27	0.37
I_{2D_2}/I_G	0.42	0.22	0.22	0.36	0.25
I_{2D}/I_G	0.63	0.39	0.43	0.63	0.62
I_{2D}^*/I_G			0.24		

TABLE II. Amplitude ratios of 2D and G peaks, * notes the single Lorentzian fit.

Previous studies suggest that the number of layers can be extracted from this ratio^{20,22,60}. Several other effects, including the substrate (coupling-effect), the strain or compression, the way of preparation, the type and quality of the solvent and the wavelength of laser excitation also affects the 2D to G Raman signal ratio. Therefore the ratio of I_{2D}/I_G has to be treated with care. The ratio in case of mechanically exfoliated and CVD samples on substrates is greater than one. For free-standing graphene and wet exfoliated species always lower than one. Taking into account the previous considerations, wet exfoliated material is structurally more similar to free-standing graphene than the ones on substrates. The substrate may generate an extra damping for the G band phonons, which can lower the intensity of the G peak and change the ratio.

B. Electron Spin Resonance spectroscopy

ESR spectra of the investigated materials are presented in Fig. 2. All samples (including the SGN18 starting material) show a narrow feature with a characteristic, uniaxial g -factor

anisotropy lineshape shown in the inset of Fig. 2. This signal most probably comes from defects which are embedded in the sp^2 matrix of graphene, which may explain the uniaxial nature of the g -factor anisotropy.

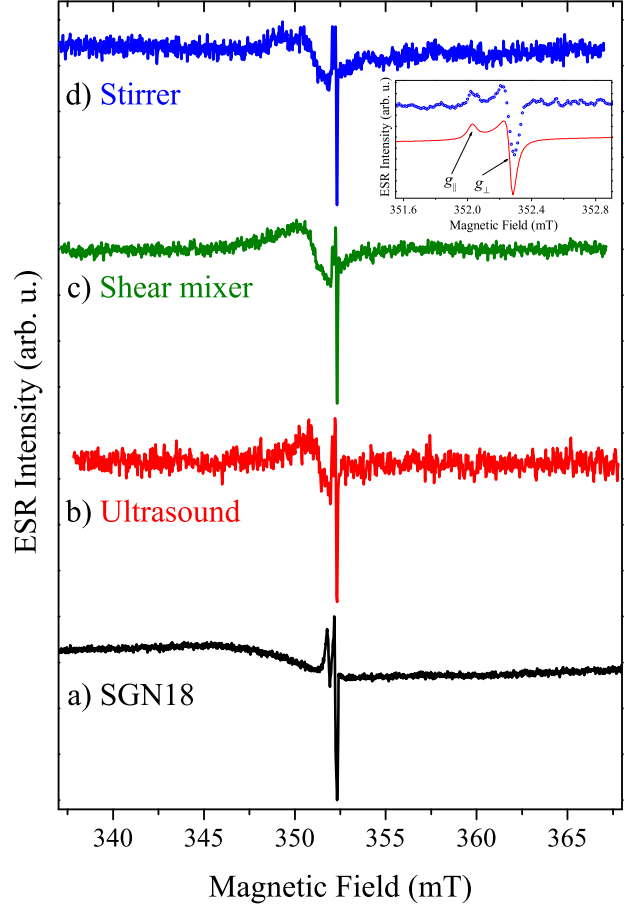


FIG. 2. ESR spectra of a) SGN18 graphite powder, b) ultrasounded, c) shear mixed, and d) stirred FLGs. The graphite powder has a broad line of about 12.2 mTs as expected at a g -factor of 2.0148. Ultrasounded FLG present a Lorentzian of 1.1 mT linewidth at $g = 2.0059$, the shear mixed present a 1.4 mT at $g = 2.0082$. The stirred material has a uniaxial anisotropic line with the width of 1.2 mT at $g = 2.0094$. The narrow uniaxial anisotropic line is coming from defects and dangling bonds in all cases. The inset shows the uniaxial g -factor simulated ESR lineshape for the narrow component in the stirrer prepared sample.

The broader component for the SGN18 graphite sample has a characteristic 12 mT ESR linewidth with a g -factor of 2.0148^{61,62}. This line originates from conduction electrons present in graphite, the value of g -factor is the weighted average of the two crystalline directions ($B \parallel c$ and $B \perp c$) with g -factors of the two, which are present in HOPG^{61,63,64} with values of 2.0023 and 2.05. Here, c is the direction perpendicular to the graphene sheets. The broader component has a 1.1 – 1.4 mT linewidth for the three FLG samples with a g -factor slightly above the free-electron value $g_0 = 2.0023$. We tentatively assign this signal to a few layer graphene phase which is p -doped due to the solvent molecules. p -doping

as in AsF_5 is known to give rise to similar signals with a $g > g_0$ ⁶⁵. Ultrasounded and shear mixed materials present a single derivative Lorentzian peak with a width of 1.1 mT and 1.4 mT, respectively. The stirred sample displays a peak similar to that of graphite powder, but with a much narrower width of 1.2 mT. The g -factor of FLG materials is between the free electron and the graphite powder. The most probable explanation for this is that single layer sheets are given a g -factor close to free electrons, but screened by the few layer sheets whose g -factor is closer to graphite. The sharp lines are associated with the defects and dangling bonds. In all materials the g -factor is above the free electrons 2.0023, thus can be associated with p -type charge carriers. The spectra were simulated with derivative Lorentzian lineshapes whose parameters are given in Table 3.

Broad component	SGN18	US	SM	ST
g	2.0148	2.0059	2.0082	2.0094
ΔB (mT)	12.2	1.1	1.4	1.2
Narrow component	SGN18	US	SM	ST
g	2.0014	2.0013	2.0006	2.0013
ΔB (mT)	0.08	0.04	0.04	0.04

TABLE III. g -factor, ΔB linewidth of the measured materials.

Previous study done by Ćirić *et al*⁶⁶ on mechanically exfoliated graphene showed a 0.62 mT wide peak with a g -factor of 2.0045. On reduced GO⁶⁷ a g -factor of 2.0062 and a width of 0.25 mT was found. The solvothermally synthesized graphene⁶⁸ shows a peak with a g -factor of 2.0044 and a width of 0.04 mT. According to these studies wet exfoliated graphene species have a g -factor close to reduced graphite, but with a width close to mechanically exfoliated and solvothermally synthesized.

C. Microwave resistance

This results are presented in Fig. 3. This method is based on measuring the microwave loss due to the sample inside a microwave cavity. This contactless method is preferred when measuring resistance in powder samples, however the measured loss depends on the sample amount and morphology. It therefore provides accurate measurement of the *relative* temperature dependent resistance, however it does not allow for a direct measurement of the resistivity. The resistance is proportional to the inverse of the microwave loss and it is normalized to that of SGN18 at 25 K to get comparable results. Microscope images are presented as insets of Fig. 3. to demonstrate the difference in grain size.

All the measured materials have a semi-conducting behavior in the investigated temperature range. This behavior is usual to defective and inhomogeneous polycrystalline metals. The difference in the microwave loss in the different samples is primarily due to a difference in the grain size. The loss, L , is known to scale with the average grain size as $L = \pi B_0^2 \sigma R^5 / 5$, where B_0 is the amplitude of the magnetic

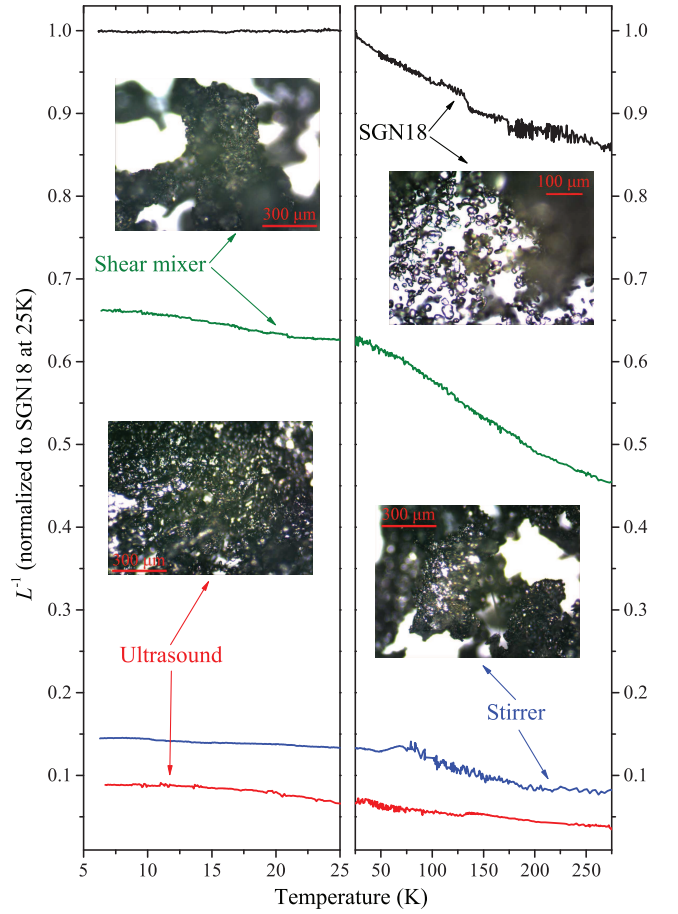


FIG. 3. Microwave resistance of FLGs compared to graphite. Insets are microscope images of the materials. Note the different scale for the SGN18 graphite sample. The different resistance of FLG species can be explained with the different grain size.

field, σ is the conductivity, and R is the average radius of the grains^{55,69}. The average grain size was obtained as about 3–5 millimeters, 500 μm , and 300 microns for the ultrasounded, stirred and shear mixed samples, respectively, by analyzing the corresponding microscope images. The trend in the microwave loss between the different samples is thus found to follow the grain size.

IV. CONCLUSIONS

We studied the vibrational, magnetic and transport properties of mechanically different post processed few layer graphene systems with Raman, ESR spectroscopy and microwave resistance measurements respectively. According to the results, processed treatment does affect the investigated properties of the material. From our results one can figure out that ultrasound treatment ends up with the best results in a meaning that this is the closest to a true single layer graphene, high quality and produced by a bulk synthesis method.

V. ACKNOWLEDGEMENT

Work supported by the European Research Council Grant No. ERC-259374-Sylo. J. C. and S. R. acknowledge the DRS POINT-2014 Founding, P. Sz., B. N. and L. F. acknowledge

the support of the Swiss National Science Foundation. The authors thank the Deutsche Forschungsgemeinschaft (DFG-SFB 953 "Synthetic Carbon Allotropes", Project A1) for financial support. The research leading to these results has received partial funding from the European Union Seventh Framework Programme under grant agreement no. 604391 Graphene Flagship.

- ¹ H. W. KROTO, J. R. HEATH, S. C. O'BRIEN, R. F. CURL, and R. E. SMALLEY, *Nature* **318**, 162 – 163 (1985).
- ² S. IIJIMA, *Nature* **354**, 56 – 58 (1991).
- ³ K. S. NOVOSELOV, A. K. GEIM, S. V. MOROZOV, D. JIANG, Y. ZHANG, S. V. DUBONOS, I. V. GRIGORIEVA, and A. A. FIRSOV, *Science* **306**, 666–669 (2004).
- ⁴ A. K. GEIM and K. S. NOVOSELOV, *Nature Materials* **6**, 183 – 191 (2007).
- ⁵ A. K. GEIM, *Science* **324**, 1530–1534 (2009).
- ⁶ A. H. C. NETO, F. GUINEA, N. M. R. PERES, K. S. NOVOSELOV, and A. K. GEIM, *Reviews of Modern Physics* **81**, 109–162 (2009).
- ⁷ B. JAYASENA and S. SUBBIAH, *Nanoscale Research Letters* **6**(1), 95 (2011).
- ⁸ C. BERGER, Z. SONG, X. LI, X. WU, N. BROWN, C. NAUD, D. MAYOU, T. LI, J. HASS, A. N. MARCHENKOV, E. H. CONRAD, P. N. FIRST, and W. A. DE HEER, *Science* **312**, 1191–1196 (2006).
- ⁹ S. Y. ZHOU, G. H. GWEON, A. V. FEDOROV, P. N. FIRST, W. A. DE HEER, D. H. LEE, F. GUINEA, A. H. C. NETO, and A. LANZARA, *Nature Materials* **6**, 770 – 775 (2007).
- ¹⁰ P. W. SUTTER, J. I. FLEGE, and E. A. SUTTER, *Nature Materials* **7**, 406 – 411 (2008).
- ¹¹ A. N. OBRAZTSOV, E. A. OBRAZTSOVA, A. V. TYURNINA, and A. A. ZOLOTUKHIN, *Carbon* **45**, 2017–2021 (2007).
- ¹² A. MALESEVIC, R. VITCHEV, K. SCHOUTEDEN, A. VOLODIN, L. ZHANG, G. V. TENDELOO, A. VANHULSEL, and C. V. HAESENDONCK, *Nanotechnology* **19**, 305604 (2008).
- ¹³ K. S. KIM, Y. ZHAO, H. JANG, S. Y. LEE, J. M. KIM, K. S. KIM, J. H. AHN, P. KIM, J. Y. CHOI, and B. H. HONG, *Nature Letters* **457**, 706–710 (2009).
- ¹⁴ A. N. OBRAZTSOV, *Nature Nanotechnology* **4**, 212–213 (2009).
- ¹⁵ A. REINA, X. JIA, J. HO, D. NEZICH, H. SON, V. BULOVIC, M. S. DRESSELHAUS, and J. KONG, *Nano Letters* **9**(1), 30–35 (2009).
- ¹⁶ C. MATTEVI, H. KIMA, and M. CHHOWALLA, *Journal of Materials Chemistry* **21**, 3324–3334 (2011).
- ¹⁷ Q. YU, L. A. JAUREGUI, W. WU, R. COLBY, J. TIAN, Z. SU, H. CAO, Z. LIU, D. PANDEY, D. WEI, T. F. CHUNG, P. PENG, N. P. GUISINGER, E. A. STACH, J. BAO, S. S. PEI, and Y. P. CHEN, *Nature Materials* **10**, 443–449 (2011).
- ¹⁸ C. C. CHEN, W. BAO, J. THEISS, C. DAMES, C. N. LAU, and S. B. CRONIN, *Nano Letters* **9**(12), 4172–4176 (2009).
- ¹⁹ A. C. FERRARI, J. C. MEYER, V. SCARDACI, C. CASIRAGHI, M. LAZZERI, F. MAURI, S. PISCANEC, D. JIANG, K. S. NOVOSELOV, S. ROTH, and A. K. GEIM, *Physical Review Letters* **97**, 187401 (2006).
- ²⁰ A. DAS, B. CHAKRABORTY, and A. K. SOOD, *Bull. Mater. Sci.* **31**(3), 579–584 (2008).
- ²¹ C. FAUGERAS, A. NERRIERE, and M. POTEMSKI, *Applied Physics Letters* **92**, 011914 (2008).
- ²² J. TSURUMI, Y. SAITO, and P. VERMA, *Chemical Physics Letters* **557**, 114–117 (2013).
- ²³ C. GOMEZ-NAVARRO, R. T. WEITZ, A. M. BITTNER, M. SCOLARI, A. MEWS, M. BURGHARD, and K. KERN, *Nano Letters* **7**(11), 3499–3503 (2007).
- ²⁴ Z. OSVÁTH, A. DARABONT, P. NEMES-INCZE, E. HORVÁTH, Z. E. HORVÁTH, and L. P. BIRÓ, *Carbon* **45**, 3022–3026 (2007).
- ²⁵ S. STANKOVICH, D. A. DIKIN, R. D. PINER, K. A. KOHLHAAS, A. KLEINHAMMES, Y. JIA, Y. WU, S. T. NGUYEN, and R. S. RUOFF, *Carbon* **45**, 1558–1565 (2007).
- ²⁶ G. EDA, G. FANCHINI, and M. CHHOWALLA, *Nature Letters* **3**, 270–274 (2008).
- ²⁷ S. PARK and R. S. RUOFF, *Nature Nanotechnology* **4**, 217–224 (2009).
- ²⁸ D. R. DREYER, S. PARK, C. W. BIELAWSKI, and R. S. RUOFF, *Chemical Society Reviews* **39**, 228–240 (2010).
- ²⁹ Y. SHAO, J. WANG, M. ENGELHARD, C. WANG, and Y. LIN, *Journal of Materials Chemistry* **20**, 743–748 (2010).
- ³⁰ J. ZHANG, H. YANG, G. SHEN, P. CHENG, J. ZHANG, and S. GUO, *Chem. Commun.* **46**, 1112–1114 (2010).
- ³¹ W. CHEN, L. YAN, and P. R. BANGAL, *Carbon* **48**, 1146–1152 (2010).
- ³² W. CHEN, L. YAN, and P. R. BANGAL, *J. Phys. Chem* **114**, 19885–19890 (2010).
- ³³ S. PEI, J. ZHAO, J. DU, W. REN, and H. M. CHENG, *Carbon* **48**, 4466–4474 (2010).
- ³⁴ E. C. SALAS, Z. SUN, A. LÜTTGE, and J. M. TOUR, *Carbon* **48**, 4466–4474 (2010).
- ³⁵ S. PEI and H. M. CHENG, *Carbon* **50**, 3210–3228 (2012).
- ³⁶ S. EIGLER, C. DOTZER, and A. HIRSCH, *Carbon* **50**, 3666–3673 (2012).
- ³⁷ S. EIGLER, M. ENZELBERGER-HEIM, S. GRIMM, P. HOFMANN, W. KROENER, A. GEWORSKI, C. DOTZER, M. RCKERT, J. XIAO, C. PAPP, O. LYTKEN, H. P. STEINRCK, P. MÜLLER, and A. HIRSCH, *Adv. Mater.* **25**, 3583–3587 (2013).
- ³⁸ S. EIGLER, S. GRIMM, M. ENZELBERGER-HEIM, P. MÜLLER, and A. HIRSCH, *Chem. Commun.* **49**, 7391–7393 (2013).
- ³⁹ S. EIGLER and A. HIRSCH, *Angewandte Chemie* **53**, 7720–7738 (2014).
- ⁴⁰ S. EIGLER, F. HOF, M. ENZELBERGER-HEIM, S. GRIMM, P. MÜLLER, and A. HIRSCH, *J. Phys. Chem. C* **118**(14), 7698–7704 (2014).
- ⁴¹ Y. HERNANDEZ, V. NICOLOSI, M. LOTYA, F. M. BLIGHE, Z. SUN, S. DE, I. T. MCGOVERN, B. HOLLAND, M. BYRNE, Y. K. GUN'KO, J. J. BOLAND, P. NIRAJ, G. DUESBERG, S. KRISHNAMURTHY, R. GOODHUE, J. HUTCHISON, V. SCARDACI, A. C. FERRARI, and J. N. COLEMAN, *Nature Nanotechnology* **3**, 563–568 (2008).
- ⁴² C. VALLÉS, C. DRUMMOND, H. SAADAoui, C. A. FURTADO, M. HE, O. ROUBEAU, L. ORTOLANI, M. MONTHIOUX, and A. PÉNICAUD, *J. Am. Chem. Soc.* **130**(47), 15802–15804 (2008).

- ⁴³ J. M. ENGLERT, J. ROÖHRL, C. D. SCHMIDT, R. GRAUPNER, M. HUNDHAUSEN, F. HAUKE, and A. HIRSCH, *Adv. Mater.* **21**, 4265–4269 (2009).
- ⁴⁴ M. LOTYA, Y. HERNANDEZ, P. J. KING, R. J. SMITH, V. NICOLASI, S. KARLSSON, F. M. BLIGHE, S. DE, Z. WANG, I. T. MCGOVERN, G. S. DUESBERG, and J. N. COLEMAN, *J. Am. Chem. Soc.* **131**, 3611–3620 (2009).
- ⁴⁵ J. M. ENGLERT, C. DOTZER, G. YANG, M. SCHMID, C. PAPP, J. M. GOTTFRIED, H. P. STEINRÜCK, E. SPIECKER, F. HAUKE, and A. HIRSCH, *Nature Chemistry* **3**, 279–286 (2011).
- ⁴⁶ A. CATHELIN, C. VALLEÉS, C. DRUMMOND, L. ORTOLANI, V. MORANDI, M. MARCACCIO, M. IURLO, F. PAOLUCCI, and A. PÉNICAUD, *Chem. Commun.* **47**, 5470–5472 (2011).
- ⁴⁷ J. M. ENGLERT, K. C. KNIRSCH, C. DOTZER, B. BUTZ, F. HAUKE, E. SPIECKER, and A. HIRSCH, *Chem. Commun.* **48**, 5025–5027 (2012).
- ⁴⁸ A. CATHELIN, L. ORTOLANI, V. MORANDI, M. MELLEFRANCO, C. DRUMMOND, C. ZAKRIAB, and A. PÉNICAUD, *Soft Matter* **8**, 7882–7887 (2012).
- ⁴⁹ T. KUILAA, S. BOSEA, A. K. MISHRAB, P. KHANRAA, N. H. KIMC, and J. H. LEE, *Progress in Materials Science* **57**, 1061–1105 (2012).
- ⁵⁰ J. COLEMAN, *Acc. Chem. Res.* **46**(1), 14–22 (2013).
- ⁵¹ A. HIRSCH, J. M. ENGLERT, and F. HAUKE, *Acc. Chem. Res.* **46**(1), 87–96 (2013).
- ⁵² P. VECERA, K. EDELTHALHAMMER, F. HAUKE, and A. HIRSCH, *Phys. Status Solidi B* **251**, 2536–2540 (2014).
- ⁵³ P. VECERA, J. C. CHACÓN-TORRES, S. REICH, F. HAUKE, and A. HIRSCH, *in preparation* (2015).
- ⁵⁴ G. FÁBIÁN, C. KRAMBERGER, A. FRIEDRICH, F. SIMON, and T. PICHLER, *Review of Scientific Instruments* **82**, 023905 (2011).
- ⁵⁵ O. KLEIN, S. DONOVAN, M. DRESSEL, and G. GRÜNER, *International Journal of Infrared and Millimeter Waves* **14**(12), 2423–2456 (1993).
- ⁵⁶ S. DONOVAN, O. KLEIN, M. DRESSEL, K. HOLCZER, and G. GRÜNER, *International Journal of Infrared and Millimeter Waves* **14**(12), 2459–2487 (1993).
- ⁵⁷ B. NEBENDAHL, D. N. PELIGRAD, M. POZEK, A. DULCIC, and M. MEHRING, *Review of Scientific Instruments* **72**, 1876–1881 (2001).
- ⁵⁸ C. THOMSEN and S. REICH, *Physical Review Letters* **85**(24), 5214–5217 (2000).
- ⁵⁹ Y. WANG, D. C. ALSMEYER, and R. L. MCCREERY, *Chem. Mater.* **2**, 557–563 (1990).
- ⁶⁰ Z. H. NI, T. YU, Z. Q. LUO, Y. Y. WANG, L. LIU, C. P. WONG, J. MIAO, W. HUANG, and Z. X. SHEN, *ACS Nano* **3**(3), 569 – 574 (2009).
- ⁶¹ D. L. HUBER, R. R. URBANO, M. S. SERCHELI, and C. RETTORI, *Phys. Rev. B* **70**, 125417 (2004).
- ⁶² M. GALAMBOS, G. FÁBIÁN, F. SIMON, L. ČIRIĆ, L. FORRÓ, L. KORECZ, A. ROCKENBAUER, J. KOLTAI, V. ZÓLYOMI, A. RUSZNYÁK, J. KÜRTI, N. M. NEMES, B. DÓRA, H. PETERLIK, R. PFEIFFER, H. KUZMANY, and T. PICHLER, *Phys. Status Solidi B* **246**(11–12), 2760–2763 (2009).
- ⁶³ M. SERCHELI, Y. KOPELEVICH, R. R. DA SILVA, J. H. S. TORRES, and C. RETTORI, *Physica B* **320**, 413–415 (2002).
- ⁶⁴ M. SERCHELI, Y. KOPELEVICH, R. R. DA SILVA, J. H. S. TORRES, and C. RETTORI, *Solid State Communications* **121**, 579–583 (2002).
- ⁶⁵ M. S. DRESSELHAUS and G. DRESSELHAUS, *Advances in Physics* **30**, 1–186 (1981).
- ⁶⁶ L. ČIRIĆ, A. SIENKIEWICZ, B. NÁFRÁDI, M. MIONIĆ, A. MAGREZ, and L. FORRÓ, *Phys. Status Solidi B* **246**(11–12), 2558–2561 (2009).
- ⁶⁷ L. ČIRIĆ, A. SIENKIEWICZ, R. GAÁL, J. JAĆIMOVIĆ, C. VÂJU, A. MAGREZ, and L. FORRÓ, *Phys. Rev. B* **86**, 195139 (2012).
- ⁶⁸ B. NÁFRÁDI, M. CHOUCAIR, and L. FORRÓ, *Carbon* **74**, 346–351 (2014).
- ⁶⁹ H. KITANO, R. MATSUO, K. MIWA, A. MAEDA, T. TAKENOBU, Y. IWASA, and T. MITANI, *Phys. Rev. Letters* **88**(9), 096401 (2002).